Eur. Phys. J. C 10, 143–151 (1999)
Digital Object Identifier (DOI) 10.1007/s100529900072

THE EUROPEAN PHYSICAL JOURNAL C

On the polarization of the nucleon sea in the meson-cloud model

K.G. Boreskov, A.B. Kaidalov

ITEP, B.Cheremushkinskaya 25, 117259 Moscow, Russia

Received: 30 October 1998 / Revised version: 4 February 1999 / Published online: 15 July 1999

Abstract. We show that the meson-cloud model predicts a substantial polarization of the sea quarks of the nucleon, because of the interference of π and ρ exchanges. This polarization is strongly flavour-dependent. The model gives an explanation of the strong increase in the structure function g_1 that has isospin $I = 1$ at small x.

1 Introduction

Experimental studies of nucleon structure functions have revealed several interesting and unexpected features. Investigation of the Gottfried sum rule by the NMC Collaboration [1] has led to the conclusion that $\bar{u}$- and $\bar{d}$-quark distributions in the proton are different. This result has been confirmed by measurements of the Drell–Yan process [2,3]. The difference between $\bar{u}$ and $\bar{d}$ distributions is measured now as a function of x [3], and is concentrated in the region of $x \lesssim 0.2$. This phenomenon has a natural explanation [4]–[6] in the meson-cloud model (Fig. 1) if positive pions in the cloud prevail over negative ones (i.e., if the contribution of the diagram of Fig. 1a is larger than the one of Fig. 1b).

In this paper, we want to pay attention to another interesting problem, the unusual small-x behaviour of the spin-structure function g_1 of protons and neutrons [7]–[12]. The situation is especially evident in the case of the neutron structure function g_1^n, which is very small in the region of $x \gtrsim 0.2$, and goes to rather large negative values as x decreases to $x \sim 10^{-2}$ [11]. This behaviour cannot be explained by valence-quark models, first since valence quarks contribute to the function g_1 mainly at $x \gtrsim 0.1$ and second, because of strong cancellation of the valence-quark contribution for the neutron[1]. At the same time, the observed small-x behaviour contradicts the one expected for the A_1 Regge-pole exchange, because of its low intercept. It would be natural to attribute this to the manifestation of the nucleon sea. However, it is usually believed that the meson-cloud model cannot lead to a polarization of sea quarks [13], because the diagrams of Fig. 1 with $\pi\pi$ exchange in the t channel do not contribute to the function g_1. In this paper we would like to emphasize that an interference between π and ρ exchanges ($\pi\rho$ exchange in the t channel, Fig. 2) leads to a substantial polarization of the nucleon structure function g_1 with isospin $I = 1$ in the t channel. It will be shown also that flavour asymmetry of the polarized-quark sea must be even stronger than that for the unpolarized case. Experimental tests of this model are proposed.

[1] Thus the neutron is a good laboratory for the investigation of nonvalence components of the nucleon.

2 General analysis of the small-x behaviour of the spin-dependent structure functions

Analysis of the small-x behaviour of structure functions of deep inelastic scattering on a nucleon in terms of the leading j-plane singularities was performed many years ago [14]. However, there is a controversy concerning the possibility of different contributions to functions $g_1(x)$, $g_2(x)$ [15], so we shall repeat here the main consequences of such an analysis.

The polarized structure functions $g_1(x, Q^2)$ and $g_2(x, Q^2)$ define the antisymmetrical in the μ, ν part of the amplitude of the virtual Compton scattering (see, e.g., [16,17]):

$$W_{\mu\nu}^{(A)}(q; P, S) = \frac{2m_N}{(P \cdot q)} \epsilon_{\mu\nu\rho\sigma} q^\rho \cdot \left[g_1(x, Q^2) S^\sigma + g_2(x, Q^2) S_\perp^\sigma \right] , \quad (1)$$

where q is a 4-momentum photon, $Q^2 = -q^2$, P and S are nucleon momentum and spin vectors, respectively, and

$$S_\perp^\sigma = S^\sigma - \frac{(S \cdot q) P^\sigma}{(P \cdot q)} . \quad (2)$$

The absorptive parts of the s-channel helicity amplitudes $F_{\lambda'_{\gamma^*}\lambda'_N;\lambda_{\gamma^*}\lambda_N}$ for forward $\gamma^* N$ scattering can be written in terms of the functions g_1 and g_2 as follows [14]:

$$\frac{1}{2}\left(F_{1\pm\frac{1}{2};1\pm\frac{1}{2}} - F_{-1\pm\frac{1}{2};-1\pm\frac{1}{2}} \right)$$

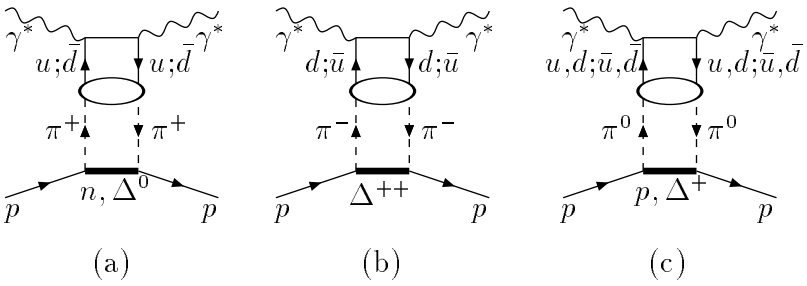

Fig. 1. Pion-exchange diagrams contributing to the structure functions F_1, F_2

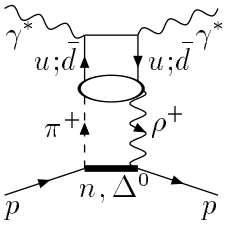

Fig. 2. $\pi\rho$ interference diagram contributing to the g_1

$$= \pm\frac{1}{m_N}\left(g_1(x,Q^2) - \frac{4m_N^2}{Q^2}x^2 g_2(x,Q^2)\right) , \qquad (3)$$

$$F_{0\mp\frac{1}{2};\pm1\pm\frac{1}{2}} = \frac{\sqrt{2Q^2}}{m_N\nu}\left(g_1(x,Q^2) + g_2(x,Q^2)\right) . \qquad (4)$$

The rules for the construction of helicity amplitudes with definite t-channel quantum numbers are well known (see, e.g., [14]). In the combination of (3) of s-channel helicity amplitudes, only states with $\sigma P = -1$ and $G(-1)^I\sigma = -1$ contribute asymptotically as $x \to 0$ (here σ represents the signature, P the parity, G the G parity and I the isospin). These are the singularities (e.g., Regge poles) of the so-called axial group. Among known Regge poles, the Reggeons A_1 ($I = 1$) and f_1 ($I = 0$) belong to this group.

The amplitude (4) corresponds to the states in the t channel, which do not have definite parity (for example Regge cuts). The rightmost singularity of this type will be a cut due to exchange of several Pomerons [2].

Let us note that Regge cuts should also obey quantum-number selection rules. In particular, Regge cuts from the exchange of any number of Pomerons in the t channel do not contribute (in the leading order in $1/x$) to the function g_1. This is due to the fact that the signature of a cut is equal to the product of signatures of exchanged Reggeons [18], and is equal to $+1$ for any number of exchanged Pomerons. So the product $G(-1)^I\sigma$ in this case equals $+1$ and does not correspond to the amplitude that we are interested in, g_1. This result can be generalized to the cuts that result from the exchange of any number of Reggeons with quantum numbers $\sigma P = +1$, $G(-1)^I\sigma = +1$ ($P, f, \omega, \rho, A_2, \ldots$) or $\sigma P = -1$, $G(-1)^I\sigma = +1$ ($\pi, \eta, \ldots$), as long as at least one of them has $I = 1$. For any pair of such Reggeons, $\sigma = \sigma_1 \times \sigma_2$, $I = I_1 + I_2$, $G = G_1 \times G_2$, and $G(-1)^I\sigma = G_1(-1)^{I_1}\sigma_1 \times G_2(-1)^{I_2}\sigma_2 = +1$.

[2] Numerically, this contribution is probably very small, for it is necessary to have at least three Pomerons, and the contribution is proportional to small spin-flip couplings of the Pomeron.

The situation is different if both Reggeons have $I_i = 1$ and both add to the total isospin $I = 1$. In this case, $I = I_1 + I_2 - 1$, and the product $G(-1)^I\sigma = -1$. So the leading-cut contributions to the small-x behaviour of g_1 are given by ρA_2, $\rho\pi$ ($I = 1$, $G = -1$). In the following, we will estimate these contributions in a simple meson-cloud model, and will show that these contributions (especially the $\pi\rho$ one) can be important in the preasymptotic region $10^{-2} \le x \le 0.1$.

Let us emphasize here that this classification of leading j-plane singularities is valid in the leading $(1/x)$ approximation, and that contributions damped by an extra x factor do not satisfy these selection rules. For example, gluonic ladders can contribute to g_1 with $I = 0$ at small x. In the following we will consider only the leading contributions for the $I = 1$ case.

3 The meson-cloud model

It has been known for a long time that π exchange plays an important role in the dynamics of peripheral inelastic interactions of hadrons (for review, see, for example, [19]–[21]). In a series of papers [19,20,22,4,6] the model with "effective" Reggeized pion exchange, which takes into account a contribution of other exchanges (ρ, A_2, etc.), has been developed and applied to a broad class of exclusive and inclusive processes in hadronic interactions. It is demonstrated that the model reproduces many characteristic features of these processes over a wide region of energy. We mention here two qualitative effects which are relevant to this subject.

It has been shown [22] that the model leads to the nontrivial behaviour of spin-dependent residues for the leading Regge poles: a small flip-nonflip ratio for $I = 0$ Reggeons (P, f), and a large one for $I = 1$ exchange (ρ Reggeon), in agreement with experimental observations. Note that the specific spin and isospin structure of the bottom blob in Fig. 1, due to pion quantum numbers, plays a crucial role in the description of the observed spin structure. There is a strong cancellation between contributions of the nucleon and Δ-isobar intermediate states for particular amplitudes.

Another example is related to the flavour structure of the nucleon quark sea mentioned in the introduction. It was first noted by Sullivan [23] that π exchange can contribute to deep inelastic scattering (DIS) (Fig. 1). In [4,6] the effective pion-exchange model has been applied to the

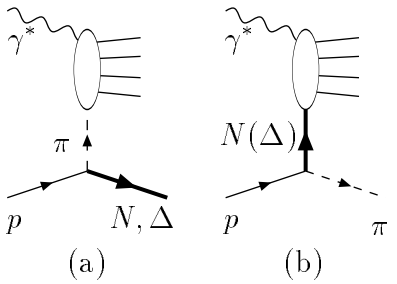

Fig. 3. Scattering of a virtual photon **a** on a pion cloud of a nucleon and **b** on a "core" baryon

calculation of antiquark distributions in a nucleon, using the distribution of $\bar{q}$ in the pion. It was noted (see also [5]) that in this model, $\bar{d}$ and $\bar{u}$ distributions in a nucleon are generally different. This difference is connected with the relative contributions of the nucleon and Δ-isobar intermediate states.

The distribution of antiquarks in the nucleon has a simple probabilistic interpretation in this model; one can use a convolution of the probability $w_{\pi^k/N}$ to find a pion π^k in a nucleon N, and the probability $\bar{q}_{\pi^k}$ to find an antiquark in the pion. Summing over all types of pions [4, 6], we have:

$$\bar{q}_N(x) = \sum_k \int_x^1 \frac{\mathrm{d}x_\pi}{x_\pi}\, w_{\pi^k/N}(x_\pi)\, \bar{q}_{\pi^k}(x/x_\pi)\ . \qquad (5)$$

The probability $w_{\pi^k/N}(x_\pi)$ is the sum of probabilities $w_k^{(R)}(x_\pi)$ of the production of a given state $R = N, \Delta$. The latter can be expressed in terms of known πNN, $\pi N\Delta$ couplings and form factors $G_\pi^R(t)$, which determine pion off-shell dependences:

$$w_k^{(R)}(x_\pi) = \frac{x_\pi}{16\pi^2} \int_{-\infty}^{\tau_R(x_\pi)} g^2_{\pi^k NR}(t) \left(G_\pi^R(t)\right)^2\ , \quad (R = N, \Delta)\ . \qquad (6)$$

Here τ_R is a minimal momentum transfer to the baryon R,

$$\tau_R(x_\pi) \approx -\frac{m_R^2 x_\pi}{1 - x_\pi} + m_N^2 x_\pi\ , \qquad (7)$$

and t is related to τ_R and the transverse momentum of produced baryon $\mathbf{k}_\perp$:

$$t \approx \tau_R - \frac{\mathbf{k}_\perp^2}{1 - x_\pi}\ . \qquad (8)$$

Besides corresponding coupling constants, the functions $g_{\pi^k NR}(t)$ contain traces over baryon indices also, providing extra t dependence of the bottom blob.

These formulas correspond to the simple pion-cloud model; in this model, there is a cloud of pions in a fast-moving nucleon, and a virtual photon interacts with an antiquark (or quark) of the pion. In this formulation the pion is an effective one and other exchanges are taken into account by a proper choice of form factors $G_R(t)$. A formulation of the meson-cloud model in terms of light-cone pion wave functions (and other pseudoscalar and vector mesons) in a nucleon [3] has been used by several authors [24–28, 13, 29–31, 21] and has been applied to different aspects of DIS, including the "spin crisis" [13,31]. However, the main attention is paid to a calculation of the function $g_1(x, Q^2)$ that results not from a meson cloud but from a "core" baryon, because the diagrams (Fig. 1) do not contribute to $g_1(x, Q^2)$. It has been shown [13] that the existence of the meson cloud leads to a substantional modification of the polarized-quark contributions in the region $x \sim 1$ (mainly due to renormalization of the nucleon wave function), but the interaction with the core baryon (the diagrams of Fig. 3b) does not influence the polarization of antiquarks from the nucleon sea.

The experience of dealing with the pion exchange model has shown that, if the pion exchange is not forbidden for a particular process, it dominates. The reason for this is related to the smallness of the pionic mass, and therefore to the close position of the corresponding pole to the physical region of the process. Unfortunately, as was shown in Sect. 2, the $\pi\pi$ exchange does not contribute to the amplitude connected to the g_1 structure function. Here we would like to consider a new contribution of the diagram of Fig. 2, one that contains $\pi\rho$ exchange in the t channel and corresponds to an interference between π and ρ exchanges[4]. According to the general classification given in Sect. 2, such a state can contribute to the small-x limit of function g_1, with the total isospin I equaling 1 in the t channel. This means that its contributions to the g_1 of protons and neutrons have different signs. The new element of this model is a strong polarization of a nucleon sea and, in particular, of antiquarks of the nucleon. We will show below that this polarization is strongly flavour - dependent.

Let us note here that the model gives a nonperturbative input for the initial conditions of QCD evolution. Thus its predictions should be valid at values of $Q^2 \sim 1$ GeV^2; they will be modified by perturbative effects at much larger Q^2.

[3] It is worth emphasizing at this point that, in contrast to the light-cone approach, we do not consider the meson cloud in terms of a relativistic wave function. This means that interactions with the meson and the "bare" nucleon (or Δ isobar) in Figs. 3a,3b are not considered as interactions with the two components of the physical nucleon. We treat these diagrams as Reggeon exchanges, and the main preference of the pion exchange is connected to the smallness of the pion mass and therefore to the close position of the corresponding pole to the physical region. The t-dependent residue of the Regge-pole amplitude can be interpreted as a form factor function describing off-shell behaviour of pionic amplitudes. In the relativistic wave-function approach, mesonic couplings are described in terms of $x, p_\perp$ dependence of the wave function, and as a result, one has exponential damping for $x_\pi \to 0$, where pion-exchange dominance is well justified and confirmed by experiments.

[4] Note that since our parameterization of the pion exchange partly contains the A_2 contribution, we effectively take into account the $A_2 - \rho$ cut also.

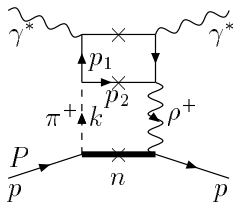

$+ (\pi \Leftrightarrow \rho) +$ interaction with antiquark

Fig. 4. The $\pi\rho$-exchange diagram with a quark box

4 Description of the model

Let us consider the diagrams of Fig. 4 to estimate the $\pi\rho$-exchange contribution to the g_1 structure function.

As we are interested in the imaginary part of the amplitude, the particles of interest in the intermediate state are on the mass shell. In order to get the partonic interpretation for the contribution of these diagrams, it is convenient to use the light-cone variables for momenta in the top part of the diagram, and to choose a Lorentz frame with a zero "plus component" of the photon momentum, $q^+ \equiv q_0 + q_z = 0$. This choice allows us to avoid non-partonic contributions [32]. In the Lorentz frame, where the proton is moving along the z axis, one has the simple kinematic relations

$$S_\perp^+ = 0 \ , \quad 2(P\cdot q) = P^+ q^- \ ,$$

and the tensor $W_{\mu\nu}$ from (1) is determined at $\mu = x$ and $\nu = y$ only by the g_1 structure function:

$$W_{xy}^{(A)} = 4 g_1(x, Q^2) \ , \quad (\text{for } q_+ = 0) \ . \tag{9}$$

A standard consideration of the upper blob (see, e.g., [17]) reduces the answer, after antisymmetrization in the photon polarization indices μ, ν to the calculation of the matrix element for the axial current component $A^+ = \gamma_5\gamma_+$ between pion and ρ meson states. The off-shell part of the quark propagator (the 'instantaneous' component [32]) is proportional to $\gamma^+ = \gamma_0 + \gamma_3$ and, since $\gamma_+^2 = 0$, it is possible for the 'plus'-component of the current to consider the struck quark as being on the mass shell as it is supposed in the partonic picture. This prescription corresponds to the light-front formalism [32].

Since the axial curent A^+ measures the helicity of the (on-shell) quark or antiquark:

$$\bar u_{p,\lambda}\gamma^+\gamma_5 u_{p,\lambda} = -\bar v_{p,\lambda}\gamma^+\gamma_5 v_{p,\lambda} = 4\lambda p^+ \ , \tag{10}$$

the result is expressed through the difference of contributions for quarks of opposite helicities, i.e., doubled contribution to the $\pi\rho$-interference term from the quark with positive helicity, as is shown schematically in Fig. 5.

For the whole diagram, one gets the well-known relations

$$g_1(x) = \frac{1}{2}\sum_q \mathrm{e}_q^2 \Delta q_N(x) \ ,$$
$$\Delta q_N(x) = q_N^+(x) - q_N^-(x) - \bar q_N^+(x) + \bar q_N^-(x) \ , \tag{11}$$

which connect the $g_1(x)$ structure function and the difference of the polarized-quark distributions $\Delta q_N(x)$, and the part of the difference due to $\pi\rho$ interference has a form similar to (5) :

$$\Delta q_N(x) = \sum_k \int_x^1 \frac{\mathrm{d}x_\pi}{x_\pi}\, w_{\pi\rho}^\alpha(x_\pi)\, \Delta q_{\pi\rho}^\alpha(x/x_\pi) \ . \tag{12}$$

Here α is a Lorentz vector index of the exchanged ρ meson (we omit indices specifying charges of π, ρ mesons); $w_{\pi\rho}^\alpha$ includes, in analogy with (6), the contribution $B_{\pi\rho}^\alpha(t)$ from the bottom (nucleon) blob of the diagram of Fig. 4 for positive helicity of the initial nucleon and meson form factors $G_{\pi,\rho}^R(t)$ (propagators and off-shell factors):

$$w_{\pi\rho}^\alpha(x_\pi) = \frac{x_\pi}{16\pi^2}\sum_{R=N,\Delta}\int_{-\infty}^{\tau_R(x_\pi)} B_{\pi\rho}^\alpha(t)\, G_\pi^R(t)\, G_\rho^R(t) \ . \tag{13}$$

$\Delta q_{\pi\rho}^\alpha$ is a difference between polarized - quark contributions coming from the top (quark) blob.

Let us discuss now separately the main ingredients entering (12) and (13).

(i) The quark blob, $\Delta q_{\pi\rho}^\alpha$

It is convenient to write down the part coming from the upper blob in terms of internal quark variables of the meson state $x_q, \mathbf{q}_\perp$, which are related to the variables $x, \mathbf{p}_\perp$ of the struck quark through the relations

$$x_q = x/x_\pi \ , \quad \mathbf{p}_{1\perp} = x\mathbf{k}_\perp + \mathbf{q}_\perp \ . \tag{14}$$

It will be assumed in the following that the *nonpolarized* quark distributions are the same for the π and ρ mesons:

$$f_{q/\pi}(x_q, \mathbf{p_qT}) = f_{q/\rho}(x_q, \mathbf{p_qT}) = f_q(x_q, \mathbf{p_qT}) \ , \tag{15}$$

with the normalization condition

$$\int_0^1 \mathrm{d}x_q \mathrm{d}^2\mathbf{q}_\perp f_q(x_q) = 1 \ . \tag{16}$$

Then

$$\Delta q_{\pi\rho}^\alpha(x_q) = (N_\pi N_\rho)^{-1/2}\int \mathrm{d}^2 q_\perp f_q(x_q, \mathbf{p_qT}) N^\alpha \ . \tag{17}$$

Here N_π, N_ρ are normalization functions, and the function N^α contains a spin-dependent contribution corresponding to the nondiagonal $\pi\rho$ and $\rho\pi$ transition,

$$N^\alpha = N_{\pi\rho}^\alpha + N_{\rho\pi}^\alpha \ , \tag{18}$$

$$N_{\pi\rho}^\alpha = \mathrm{Tr}\left[(\hat p_1 + m_q)\frac{1-\gamma_5\hat s_1}{2}\Gamma^{(\pi)}(-\hat p_2 + m_q)\Gamma_\alpha^{(\rho)}\right] \ , \tag{19}$$

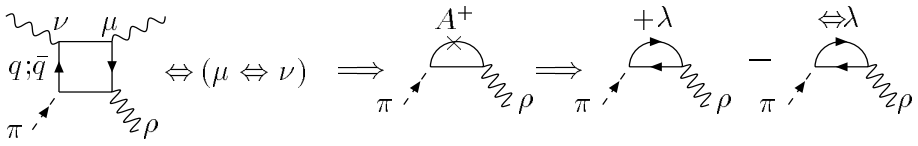

Fig. 5. Schematic reduction of the g_1 amplitude to the difference of polarized-quark distributions

(s_1 is a spin vector of the quark struck by the photon), and similarly (with interchange of π and ρ vertices) for $N^{\alpha}_{\rho\pi}$.

It is important that p_1 and p_2 in the equation above are on-mass-shell 4-momenta of the quarks, where $p_1^2 = p_2^2 = m_q^2$, and that the "minus" component of momentum is not conserved in the meson–quark–quark vertices: $p_1^- + p_2^- \neq k^-$. (These prescriptions have been accepted just at the point where the relations (10) have been used.) As a result, the following kinematic relation is valid:

$$(p_1 + p_2)^2 = M_0^2 = \frac{\mathbf{p}_{qT}^2 + m_q^2}{x(1-x)} \ , \tag{20}$$

where M_0 is a standard variable in the light-cone formalism.

The spin structure of the meson–quark vertices has been chosen as

$$\Gamma^{(\pi)} = \gamma_5 \ , \quad \Gamma^{(\rho)}_{\alpha} = \gamma_\alpha \ . \tag{21}$$

The normalization functions N_π, N_ρ can be obtained, e.g., by consideration of the diagonal electromagnetic form factors at zero-momentum transfer. This gives us

$$N_\pi = \mathrm{Tr}\left[(\hat{p_1} + m_q)\gamma_5(-\hat{p_2} + m_q)\gamma_5\right] \ , \tag{22}$$

$$N_\rho = \tfrac{1}{3}\mathrm{Tr}\left[(\hat{p_1} + m_q)\gamma_\alpha(-\hat{p_2} + m_q)\gamma_\alpha\right] \ , \tag{23}$$

for the diagonal $\pi\pi$ and $\rho\rho$ transitions, respectively. The quark mass m_q was taken as $m_q = 0.3$ GeV for calculations. We pointed out above that we estimate the large - distance contribution of the meson cloud to the function g_1, so the mass of the quark in our model should be considered as a constituent quark mass, and we take for it the value $m_q = 0.3$ GeV.

To show the important role of the choice of the distribution $f_q(x_q)$, we have tried two extreme cases: a simple wave-function description which assumes quark–antiquark content of the pion [33], and the Glück–Reya–Stratmann parameterization [34], which has a singularity at $x = 0$. The parameterizations used for calculations are listed in the appendix.

(ii) The nucleon blob, B_α

The bottom blob with $R = N, \Delta$ in the intermediate state contains the nucleon traces

$$B^{\alpha} = \sum_R (B^{(R)\alpha}_{\pi\rho} + B^{(R)\alpha}_{\rho\pi}) \ , \tag{24}$$

where

$$B^{(N)\alpha}_{\pi\rho} = \mathrm{Tr}\left[(\hat{P} + m_N)\frac{1+\hat{S}\gamma_5}{2}\Gamma_{\pi NN}\right.$$

$$\left. D^{(N)}(P-K)\Gamma^{\alpha}_{\rho NN}\right] \tag{25}$$

$$B^{(\Delta)\alpha\tau}_{\pi\rho} = \mathrm{Tr}\left[(\hat{P} + m_N)\frac{1+\hat{S}\gamma_5}{2}\Gamma^{\tau}_{\pi N\Delta}\right.$$

$$\left. D^{(\Delta)}_{\tau\sigma}(P-K)\Gamma^{\alpha\sigma}_{\rho NN}\right] \tag{26}$$

The structure of the vertices $\Gamma_{\pi NR}$ and $\Gamma_{\rho NR}$ and propagators $D^{(R)}$ is given in the appendix.

Let us note that for *unpolarized* quark sea, the contributions to the bottom blob due to the nucleon and Δ isobar in the intermediate state are comparable in magnitude. The particular values of coupling constants lead to larger values for the nucleon contribution, and as a result, the flavour asymmetry of the antiquark sea of the proton in favour of $\bar{d}$ antiquarks. It can be shown that for the *polarized* quarks, the contribution of Δ isobar is strongly suppressed due to the spin structure of the vertices. Moreover, due to C-parity limitations only exchanges of charged π, ρ mesons are allowed. The result is a much more drastic flavour asymmetry for the polarized-quark sea than that for the unpolarized one.

(iii) The form factors, $G^R_{\pi,\rho}(t)$

We have used the same π-meson form factor $G^R_\pi(t)$ as that in [4,6] which allows us to give a consistent description of nucleon and Δ inclusive spectra, data on Drell–Yan process, and some other inclusive and exclusive processes in the framework of the pion exchange model. The information about the function G^R_ρ, which describes the off-shell behaviour of the ρ-meson propagator, is much more limited[5]. We used the simple exponential damping. The formulas for the form factors are given in the appendix.

5 Comparison with experiments

The model formulated above allows us to calculate sea-quark polarization to the nucleon structure function g_1 with $I = 1$. We have not tried to calculate a nonperturbative contribution to the function g_1 with $I = 0$ (for the calculation of $\rho - \rho$ exchange for this function, see [35]). Experimental data show that at small $x \sim 10^{-2}$, the amplitude with $I = 1$ in the t channel gives the main contribution. In the following we will compare our results with the g_1 of the neutron, because in this case a contribution of the valence quarks is small, and contribution of the sea can be more easily separated than that of the proton case. The results for the g_1^p are just opposite in sign

[5] We have not used the Reggeized version for the off-shell behaviour of the ρ exchange, as it is difficult to find one which would be valid for nonsmall values of x_ρ also.

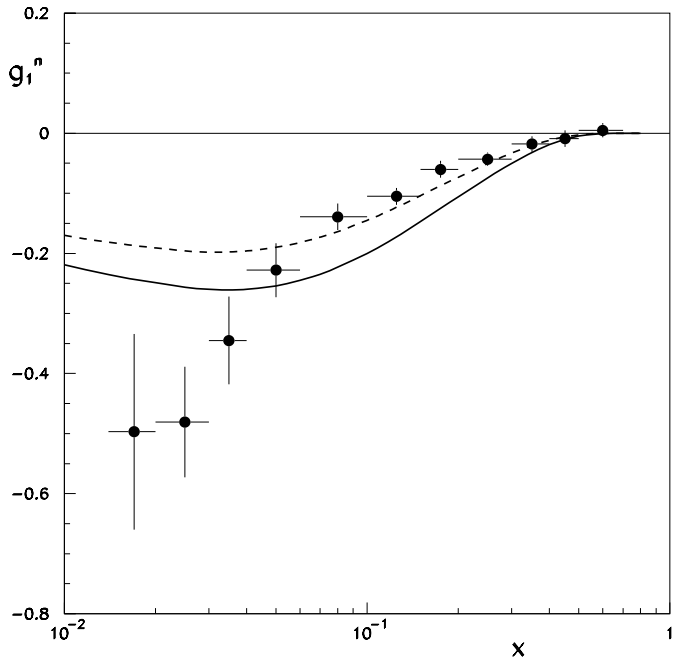

Fig. 6. Description of experimental data of the E154 Collaboration [11] on g_1^n, with $f_q(x)$ from the relativistic wave-function model [33] for two form-factor parameter values: $R^2 = 0.7$ GeV^2 (solid) and $R^2 = 1.0$ GeV^2 (dashed)

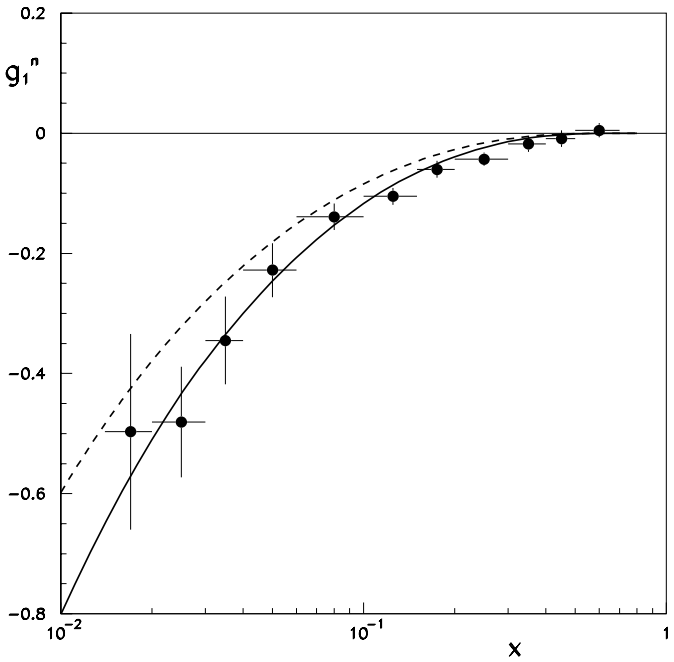

Fig. 7. Description of data [11] on g_1^n with $f_q(x)$ from the GRS parametrization [34]. The solid curve corresponds to $R^2 = 0.7$ GeV^2, and the dashed one to $R^2 = 1.0$ GeV^2

because $I = 1$ in the considered contribution. Note that gluons (in particular, the gluon anomaly [17]) do not contribute to this isospin combination. These contributions can be important for the $I = 0$ amplitude.

Our model depends on several parameters, which are not well known (e.g., the $g_{\rho NN}$ coupling constant), and on assumptions listed above. So we do not aim for detailed descriptions of the I=1 sea component of the structure function g_1, but rather for a qualitative effect, and to demonstrate that this effect is of the right order of magnitude.

In Fig. 6, the contribution of the simplest diagrams of Fig. 2 with only the $q\bar{q}$ component of the pion (ρ-meson) wave function is shown. The function g_1 decreases for $x < 5 \cdot 10^{-2}$ due to a fast decrease of the wvae functions as $x_q \to 0$. It is known, however, that the valence-quark distributions in the pion are substantially different (especially in the region of small x_q) from the behaviour corresponding to the simplest $q\bar{q}$ wave function. For a distribution of valence quarks given by the GRS model [34], we obtain theoretical curves, shown in Fig. 7, which are in a good agreement with experimental data. Thus the model gives a reasonable estimate for both the size and the form of the sea-quark polarization in the nucleon. A word of caution concerning the above estimate of the valence quarks in the pion: The small-x behaviour of the valence quarks of the pion in the GRS model $\sim 1/x^\gamma$ with $\gamma \approx 0.5$ is , strictly speaking, true only for a "diagonal" transition with quantum numbers of A_2, f in the t channel. In our case, we should know the behaviour of the analogous quantity with axial quantum numbers in the t channel. In the model in [36], where corresponding Reggeons are generated due to gluon emissions in the box diagram (Fig. 8), it is possible to show that a difference between vector and axial-vector contributions appears only at three-loop level (the emission of two gluons in the s channel of Fig. 8). So this difference should be important in the upper blob only at small $x_q < x_q^{\rm cr} \approx 0.1$. This means that our estimate with the GRV structure function of the pion can be valid up to $x \sim \bar{x}_\pi x_q^{\rm cr} \sim 0.01$. At smaller values of x, we expect a gradual transition to the behaviour corresponding to the A_1 Regge exchange.

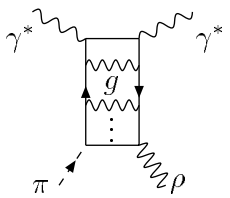

Fig. 8. Gluon ladder for $\gamma^*\pi \to \gamma^*\rho$ transition

We would like to emphasize that due to the smallness of the diagram with the Δ intermediate state of Fig. 2, only the $\bar{d}$ quarks of the proton ($\bar{u}$ quarks of the neutron) are polarized. The following relations for polarized-quark distributions in the proton and the neutron are valid in the model (here we separate quark and antiquark polarized distributions, unlike in (11)):

$$\Delta u^p_{\rm sea}(x) = \Delta d^n_{\rm sea}(x) = \Delta \bar{d}^p(x) = \Delta \bar{u}^n(x) \approx 6g_1^p(x) = -6g_1^n(x)\ , \quad (27)$$

$$\Delta d^p_{\rm sea}(x) = \Delta u^n_{\rm sea}(x) = \Delta \bar{u}^p(x) = \Delta \bar{d}^n(x) \approx 0\ . \quad (28)$$

Thus the model predicts an even higher flavour asymmetry for polarized antiquarks than for unpolarized distribu-

tions. Present estimates of polarization for antiquarks do not contradict the limits on this quantity established from a study of semi-inclusive DIS [37], especially taking into account that the hypothesis of flavour symmetry for light quarks (antiquarks) of the sea has been used in the analysis of experimental data. In principle, different flavour contributions to the polarized-quark sea can be separated, and model predictions tested, if accuracy of experimental data will be improved.

The most straightforward test of our model would be a measurement of the polarization asymmetries in DIS with simultaneous registration of a nucleon or Δ in the final state. For Δ production, sea polarization should be small or absent compared to the case of neutron production off a proton (or a proton from a neutron target).

Let us comment on the relevance of these results for the Bjorken [38] and Ellis–Jaffe [39] sum rules. It is clear from experimental results [10] that the region of $x < 0.1$, where sea quarks are important, gives a substantial contribution ($\sim 30\%$) to the Bjorken sum rule. This means that the sea-quark component of a nucleon should be important in the dynamical calculation of the axial coupling constant g_A. So all calculations of the axial couplings of baryons [31] should be reconsidered with an account of this mechanism. Another important problem for the test of the Bjorken sum rule is the evaluation of the integral of the difference $g_1^p(x) - g_1^n(x)$ in the unmeasured region of very small x [10]. The simplest power-law extrapolation of existing data gives a large contribution to the integral [10]. Our investigation indicates that a steep increase of the sea component with $I = 1$ in the structure function $g_1(x)$ should change at $x \sim 10^{-2}$ to a slower increase (or constant behaviour) as x decreases. In this case, the unmeasured small-x region contributes only 0.02/0.03 to the integral.

It is known [13,31] that the inclusion of a meson cloud in the nucleon wave function leads to better agreement with the Ellis–Jaffe sum rule. However, it is difficult to obtain a good description of experimental data on g_1^p, g_1^n and to solve completely the problem of spin crisis. We hope that this situation will improve with the account of interference diagrams considered here. An interference of K and K^* exchanges will lead to some polarization of s and $\bar{s}$ quarks, which can be relevant for this problem.

6 Conclusions

In this paper we proposed a new nonperturbative mechanism for polarization of sea quarks in a nucleon. The mechanism leads to a strong flavour dependence of the sea polarization. It can not be imitated by the diagrams of perturbative QCD. An estimate of the $\pi\rho$ interference mechanism carried out in this paper shows that it can account for the unusual behaviour of the structure function g_1^n in the small-x region and is important for calculations of the axial couplings of baryons.

Future experiments with polarized beam and target in DIS and hadronic interactions will allow a critical test of the proposed mechanism for the sea-quark polarization.

Acknowledgements. The authors thank B.L. Ioffe and J.H. Koch for helpful discussions. K.B. is grateful to the Instituto de Ciencias Nucleares, UNAM (Mexico), especially A. Turbiner, for their kind hospitality as the present work was finished. This work was supported in part by INTAS grant 93-0079ext, NATO grant OUTR.LG 971390, RFBR grants 96-02-191184a, 96-15-96740, and 98-02-17463 and DGAPA grant IN 105296.

Appendix

Here we give a description of the main components entering the model – quark distributions used for calculations, baryon vertices and propagators, and form factors.

A. Quark distributions in mesons

In order to illustrate the effect of the choice of different parametrizations, we used two types of distributions. The first one supposes that mesons contain only a valence quark and antiquark. This two-particle distribution is parametrized in terms of the light-cone wave function [33]:

$$f_q(x_q, \mathbf{p}_{qT}) = |\psi(x_q, \mathbf{p}_{qT})|^2 \ , \tag{A.1}$$

where

$$\psi(x_q, \mathbf{p}_{qT}) = \sqrt{\frac{M_0}{2x_q(1-x_q)}}\phi(p) \ , \tag{A.2}$$

with

$$M_0^2 = \frac{m_q^2 + \mathbf{p}_{qT}^2}{x_q(1-x_q)} \ , \tag{A.3}$$

$$p = \sqrt{\mathbf{p}_{qT}^2 + p_z^2} \ , \quad p_z = M_0(x_q - 1/2) \ . \tag{A.4}$$

The function $\psi(x, \mathbf{p}_T)$ is normalized as

$$\frac{1}{16\pi^3}\int \mathrm{d}x \int \mathrm{d}^2 p_T \, |\Psi(x, \mathbf{p}_T)|^2 = 1 \ , \tag{A.5}$$

which corresponds to the standard normalization of the function $\phi(p)$:

$$\frac{1}{(2\pi)^3}\int \mathrm{d}^3 p \, |\phi(p)|^2 = 1 \ . \tag{A.6}$$

We use a simple oscillator-type parametrization for the wave function $\phi(p)$ [33]:

$$\phi(p) = \pi^{-3/4}\beta^{-3/2}(2\pi)^{3/2}\exp(-p^2/2\beta^2) \tag{A.7}$$

with $\beta = 0.32$. The second type of distribution, written under an assumption of the multiparticle content of a meson, was taken from the paper by Glück, Reya and Stratmann [34]:

$$f_q(x_q, \mathbf{p}_{qT}) = 0.471 x_q^{-0.501}(1-x_q)^{0.367}(1 + 0.632\sqrt{x_q})\,\frac{\lambda}{\pi} \times \exp(-\lambda \mathbf{p}_{qT}^2) \ , \tag{A.8}$$

where the value of λ does not affect the final result, and was chosen to be equal to 1.

B. Baryon vertices

The baryon vertices were taken in the form

$$\Gamma_{\pi NN} = g_{\pi NN}\gamma_5 \ , \tag{B.1}$$

$$\Gamma^{\alpha}_{\rho NN} = g^{(0)}_{\rho NN}\gamma_\alpha + \frac{g^{(1)}_{\rho NN}}{2m_N}\sigma_{\alpha\beta}k_\beta \ , \tag{B.2}$$

$$\Gamma^{\tau}_{\pi N\Delta} = g_{\pi N\Delta}p_{N\tau} \ , \tag{B.3}$$

$$\Gamma^{\alpha\tau}_{\rho N\Delta} = g_{\rho N\Delta}\gamma_5(\hat{k}g_{\alpha\tau} - \gamma_\alpha k_\tau) \ , \tag{B.4a}$$

$$\Gamma^{\alpha\tau}_{\rho N\Delta} = g_{\rho N\Delta}\epsilon^{\alpha\tau\delta\gamma}P_\delta p^{\gamma}_{\Delta} \ , \tag{B.4b}$$

where α and τ are Lorentz indices of ρ and Δ, respectively. The form of the first three vertices is unambiguious; for the fourth one, we tried both the structure (B.4a) used in meson-exchange models [40], and the simplest structure (B.4b), which is in agreement with experimental data on the process $\pi p \to \pi\Delta$ [41].

Only the second term in (B.2) contributes to the small-x asymptotics of the $g_1(x)$. The intermediate state with Δ isobar does not contribute to the asymptotics of the $g_1(x)$ at all (for the both structures (B.4a), (B.4b)). This fact results in important predictions on flavour structure of the polarized-quark sea (see Sect. 5).

The following values of coupling constants were taken [6,40]:

$$g^2_{\pi^0 pp}/4\pi = 14.6 \ , \tag{B.5}$$

$$g^{(0)2}_{\rho^0 pp}/4\pi = 0.84 \ , \quad g^{(1)}_{\rho NN}/g^{(0)}_{\rho NN} = 6.1 \ , \tag{B.6}$$

$$g^2_{\pi^- p\Delta^{++}}/4\pi = 19 \ \mathrm{GeV}^{-2} \ , \tag{B.7}$$

$$g^2_{\rho^- p\Delta^{++}}/4\pi = 34.7 \ \mathrm{GeV} \ . \tag{B.8}$$

C. Baryon propagators

Propagators of the nucleon and the Δ isobar have standard forms for particles of spin 1/2 and 3/2:

$$D_N(P) = \hat{P} + m_N \ , \tag{C.1}$$

$$D_\Delta(P) = (\hat{P} + m_\Delta)\left[\frac{2}{3m^2_\Delta}P_\alpha P_\tau - g_{\alpha\tau} + \frac{1}{3}\gamma_\alpha\gamma_\tau + \frac{1}{3m_\Delta}(\gamma_\alpha P_\tau - \gamma_\tau P_\alpha)\right] . \tag{C.2}$$

D. Form factors

The functions $G^R_\pi(t)$ were defined using the same parameterization as in [6]:

$$G^R_\pi(t) = \exp\left[\left(R^2_{1R} + \alpha' \ln 1/x_\pi\right)(t-\mu^2)\right] \times \times \begin{cases} \pi\alpha'/(2\sin[\pi\alpha'_\pi(t-\mu^2)/2]) \ , & |t| \le |T_R| \\ \exp[R^2_{2R}(t-T_R)]\pi\alpha'_\pi & \\ \quad /2\sin[\pi\alpha'_\pi(T_R-\mu^2)/2]) \ , & |t| > |T_R| \end{cases} \tag{D.1}$$

with parameter values

$$R^2_{1N} = 0.3 \ \mathrm{GeV}^{-2}, \quad R^2_{2N} = 2.0 \ \mathrm{GeV}^{-2}, \quad T_N = -0.4 \ \mathrm{GeV}^2, \tag{D.2}$$

$$R^2_{1\Delta} = 0.2 \ \mathrm{GeV}^{-2}, \quad R^2_{2\Delta} = 0.74 \ \mathrm{GeV}^{-2}, \quad T_\Delta = -0.7 \ \mathrm{GeV}^2. \tag{D.3}$$

The values of the parameters provide continuity of the derivative of function at $t = T_R$. In fact, as was mentioned, the contribution of the Δ isobar is negligible, and only the nucleon intermediate state contributes to the g_1 structure function.

The function $G^N_\rho(t)$ was taken as a simple form consistent with meson-exchange models,

$$G^N_\rho(t) = \frac{\mathrm{e}^{R^2(t-m^2_\rho)}}{t-m^2_\rho} \ , \tag{D.4}$$

and the results of calculations with $R^2 = 0.7 \ \mathrm{GeV}^{-2}$ and $R^2 = 1.0 \ \mathrm{GeV}^{-2}$ were shown as an illustration.

References

1. P. Amaudruz, et al., Phys. Rev. Lett. **66**, 2712 (1991); M. Arneodo, et al., Phys. Rev. D **50**, R1 (1994)
2. A. Baldit, et al., Phys. Lett. B **332**, 244 (1994)
3. E.A. Hawker, et al., Phys. Rev. Lett. **80**, 3715 (1998)
4. G.G. Arakelyan, K.G. Boreskov, A.B. Kaidalov, Sov. J. Nucl. Phys. **33**, 247 (1981)
5. A.W. Thomas, Phys. Lett. B **126**, 97 (1983)
6. G.G. Arakelyan, K.G. Boreskov, preprint ITEP-50-1984, 1984; Sov. J. Nucl. Phys. **41**, 267 (1985)
7. J. Ashman, et al. (EMC), Phys. Rev. Lett. B **206**, 364 (1986); Nucl. Phys. B **328**, 1 (1989)
8. D. Adams, et al. (SMC), Phys. Lett. B **329**, 399 (1994); B **357**, 248 (1995); B **396**, 338 (1997); Phys. Rev. D **56**, 5330 (1997)
9. P.L. Anthony, et al. (E142), Phys. Rev. Lett. **71**, 959 (1993); Phys. Rev. D **54**, 6620 (1996)
10. K. Abe, et al. (E143), Phys. Rev. Lett. **74**, 346 (1995); **75**, 25 (1995); Phys. Lett. B **364**, 61 (1995); SLAC-PUB-7753 (1998)
11. K. Abe, et al. (E154), Phys. Rev. Lett. **79**, 26 (1997); Phys. Lett. B **404**, 377 (1997); Phys. Lett. B **405**, 180 (1997);
12. K. Ackerstaff, et al. (HERMES), Phys. Lett. B **404**, 383 (1997)
13. V.R. Zoller, Zeit. Phys. C **53**, 443 (1992); C **60**, 141 (1993)
14. R.L. Heimann, Nucl. Phys. B **64**, 429 (1973)
15. F.E. Close, R.G. Roberts, Phys. Lett. B **336**, 257 (1994)
16. B.L. Ioffe, V.A. Khoze, L.N. Lipatov, Hard Processes, North Holland, Amsterdam, 1984
17. M. Anselmino, A. Efremov, E. Leader, Phys. Rep. **261**, 1 (1995)
18. V.N. Gribov, Proceedings of the XII International Conference on High Energy Physics, Dubna, 1964, p. 394
19. K.G. Boreskov, A.B. Kaidalov, L.A. Ponomarev, preprint ITEP-92-1973 (1973), published in Proceedings of Yerevan Physics School, 1975

20. L.A. Ponomarev, Sov. J. Part. Nucl. **7**, 70 (1976)
21. J. Speth, A.W. Thomas, Advances in Nuclear Physics, **24**, 83 (1998)
22. K.G. Boreskov, A.A. Grigoryan, A.B. Kaidalov, I.I. Levintov, Sov. J. Nucl. Phys. **27**, 432 (1978)
23. J.D. Sullivan, Phys. Rev. D **5**, 1732 (1972)
24. E.M. Henley, G.A. Miller,Phys. Lett. B **251**, 453 (1990)
25. A. Signal, A.W. Schreiber, A.W. Thomas, Mod. Phys. Lett. A **6**, 271 (1991); W. Melnitchouk, A.W. Thomas, A.I. Signal, Zeit. Phys. **340**, 85 (1991)
26. S. Kumano, Phys. Rev. D **43**, 59; 3067 (1991)
27. W.-Y.P. Hwang, J. Speth, G.E. Brown, Zeit. Phys. A **339**, 461 (1991)
28. E. Jenkins, A.V. Manohar, Phys. Lett. B **255**, 558 (1991); B **259**, 353 (1991)
29. P.J. Mulders, A.W. Schreiber, H. Meyer, Nucl. Phys. A **549**, 498 (1992)
30. A. Szczurek, H. Holtmann, Acta Phys. Pol. B **24**, 1833 (1993)
31. H. Holtmann, A. Szczurek, J. Speth, Nucl. Phys. A **596**, 631 (1996)
32. C. Michael, F.P. Payne, Zeit. Phys. **C12**, 145 (1982)
33. W. Jaus, Phys. Rev. D **44**, 2851 (1991)
34. M. Glück, E. Reya, M. Stratmann, Zeit. Phys. C **53**, 651 (1992)
35. R.J. Fries, A. Schäfer, Phys. Lett. B **443**, 40 (1998)
36. A.A. Grigoryan, N.Ya. Ivanov, A.B. Kaidalov, Sov. J. Nucl. Phys. **36**, 867 (1982)
37. B. Adeva, et al. (SMC), Phys.Lett. B **420**, 180 (1998)
38. J.B. Bjorken, Phys. Rev. **148**, 1467 (1966); D **1**, 1376 (1970)
39. J. Ellis, R.L. Jaffe, Phys. Rev. D **9**, 1444 (1974); Erratum D **10**, 1669 (1974)
40. R. Machleidt, K. Holinde, Ch. Elster, Phys. Rep. **149**, 1 (1987)
41. A.B. Kaidalov, V.I. Zakharov, Pis'ma v JETP **2**, 192 (1966)